JOURNAL OF CATALYSIS 57, 136–146 (1979)

Acidic and Cracking Properties of Offretite

CLAUDE MIRODATOS

Institut de Recherches sur la Catalyse, 79 Boulevard du 11 Novembre 1918, 69626 Villeurbanne Cedex, France

AND

DENISE BARTHOMEUF

Laboratoire de Catalyse Organique, E.S.C.I.L., L.A. CNRS No. 231, 43 Boulevard du 11 Novembre 1918, 69621 Villeurbanne, France

Received January 27, 1978; revised October 4, 1978

The acidic and catalytic properties of offretite zeolites have been studied as a function of potassium content. NH_3 thermodesorption and ir studies of pyridine adsorption have shown that the weaker protonic acid sites arise from the exchange of the first of the three potassium cations located in gmelinite windows. The progressive removal of the last two cations creates strong acid sites and allows the reaction molecules to enter the gmelinite cages. There is evidence for two types of Lewis acidity. One of them is suggested to arise from a partial dehydroxylation during pyridine evacuation. Both Lewis sites are strong. The isooctane cracking selectivity is modified and gives a high C_3/C_4 ratio at the expense of iso C_4 when the ion content is small enough to allow a diffusion of molecules through the gmelinite cavities.

Only a few results have been published on the catalytic properties of offretite zeolite. This material has a structure consisting of channels 6.3 Å in aperture, parallel to the *c* axis, which allows hydrocarbons such as iso- and neoparaffins to enter (*1*, *2*). These channels are circumscribed by gmelinite cages with eight-membered oxygen openings in the *a* direction. These windows are large enough to admit molecules with a critical diameter of about 4.5 to 5 Å (*1*, *3*, *4*). Some of the entrances to gmelinite cages may be blocked by potassium cations up to about 1.7 K^+ per gmelinite cage (*3*). The remaining K^+ ions (one per unit cell) are located in the inaccessible cancrinite cage (*3*, *5*). A part of them is exchangeable by protons (*6*). Studies of *n*-hexane cracking have shown that a highly exchanged offretite is as active as erionite or ammonium faujasite (*1*) with a selectivity comparable to that of rare earth faujasite (*4*) (little C_3 and much C_4 hydrocarbons). Conversion of 2-methylpentane occurs extensively in offretite (*4*). Since potassium ion location may change greatly the accessibility and properties of active sites, a study was made of the influence of potassium content on the acidic and catalytic properties of offretite.

EXPERIMENTAL

Catalysts

A series of variously exchanged offretites was obtained from a TMA offretite sample

0021-9517/79/040136-11$02.00/0

TABLE 1

Chemical Composition, Thermodesorption, and Colored Indicator Results

Catalysts	Na per u.c.	K per u.c.	Peak maximum[a] T.D.	Amount evolved[b] (a.u.)	Maximum acid strength % H_2SO_4[c]
Of-3.1	0.07	3.1	205	1	48
Of-3.0	0.07	3.0			48
Of-2.4	0.03	2.4			48
Of-2.3	0.03	2.3			48
Of-2.1	0.02	2.1	225 260	5	48
Of-1.7	0.02	1.7	285	5	72
Of-1.3	0.02	1.3	shoulder 290	7	90
Of-1.1	0.01	1.1	305	8	90
Of-1.0	0.01	1.0			90
Of-0.9	0.01	0.9			90
Of-0.6	0.01	0.6	315	20	90
Of-0.4	0 01	0.4	[d]	[d]	[d]

[a] Ammonia thermodesorption (see Fig. 8).

[b] Amount of ammonia evolved deduced from the area of the 160–400°C peak in fig. 8.

[c] Acid strength evaluated as the concentration, in percent, of a sulfuric acid solution which induces color change of Hammett and arymethanol indicators.

[d] Not determined.

provided by Barrer and Harding (*3*) (TMA: tetramethylammonium). Its chemical composition was $Na_{0.07}K_{3.1}(TMA)_x(AlO_2)_{3.6}(SiO_2)_{14.4}(H_2O)_y$. Chemical exchange of cations with ammonium acetate solutions was performed as described elsewhere (*6*) and a heat treatment at 380 and 550°C for 15 hr under a dry air flow provided active acidic catalysts. The materials are designated according to the number of potassium cations per unit cell and have the chemical compositions given in Table 1. It was checked by X-ray diffraction and ir studies that except for the Of-0.4 sample they have good crystallinity.

Acidity Studies

Colored indicators. The existence of various acid strengths was detected with Hammett and arylmethanol indicators reacting with the more external sites on particles. The titration of inner sites was not possible due to the small size of the channels. It will be shown in the paper that changes in acid strength reflect changes in intraparticle acidity.

Infrared studies. Pyridine adsorption was used to characterize Brønsted and Lewis acidity. Thin wafers of zeolite (~25 mg, 2 cm in diameter) were heated at 450°C for 8 hr under a dry oxygen stream. They were then evacuated for 15 hr at 350°C. Pyridine was adsorbed at room temperature for 15 hr at 15 Torr pressure (1 Torr = 133.33 N m^{-2}). Attempts were made to adsorb pyridine at 150°C in order to check the adsorption process. No significant differences were observed.

Thermodesorption. The thermodesorption of ammonia and pyridine have been performed in a Sartorius thermobalance. The samples were evacuated at room temperature. They were then heated at 400°C for 2 hr under a pressure of 100 Torr of dry oxygen and further evacuated for 6 hr at 400°C. The reference weight was taken after cooling under vacuum at room temperature. The base was introduced at room temperature in the apparatus at 100-Torr pressure for ammonia and 15-Torr for pyridine. The adsorption was allowed to occur for 10 hr at room temperature. Some

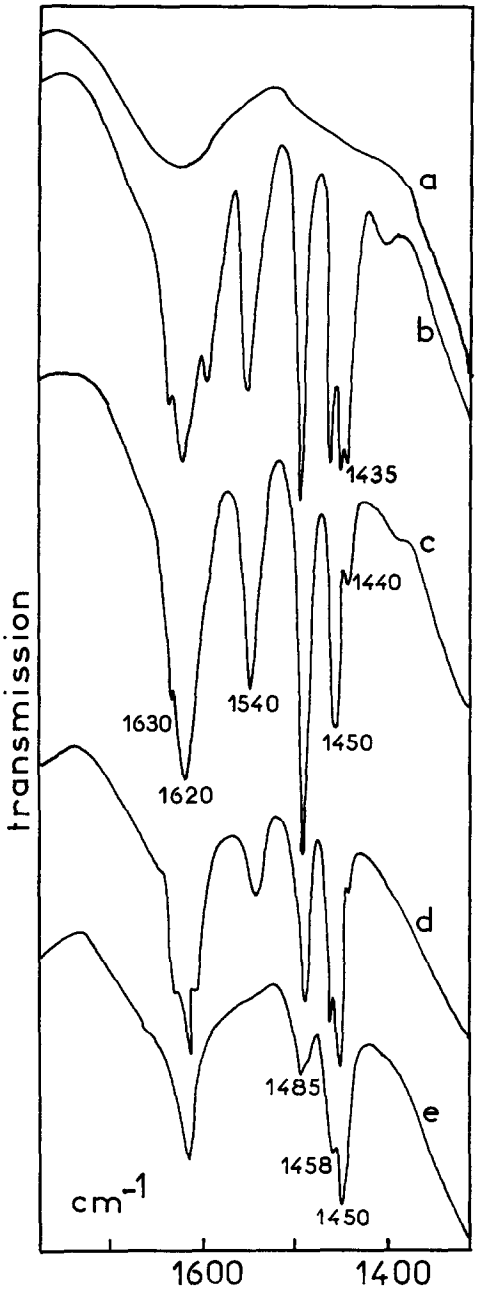

FIG. 1. Pyridine adsorption on Of-0.6 zeolite. (a) Initial spectrum; (b) pyridine adsorption at room temperature; evacuation at (c) 150, (d) 300, and (e) 400°C.

adsorption experiments were made at 150°C but gave no significant differences. Excess of base was evacuated at room temperature up to a constant weight loss (about 5 hr). The programmed thermodesorption was performed under continuous pumping with a heating rate of 8°C/min up to 400°C. The weight loss changes were recorded and moreover the flow of molecules evolved was followed with a Pirani gauge. The weight loss curves have been used to calculate, through 10°C intervals, the desorption rate in mole of base evolved per degree and per zeolite unit cell weight.

Catalytic activity. Isooctane cracking has been used to characterize the catalytic activity (*7*). The sample (10 mg) was pretreated in a microreactor for 15 hr under a hydrogen stream at 465°C. Then isooctane was introduced continuously (pressure 100 Torr) in the carrier gas. The thickness of the bed was less than 1 mm in order to avoid any channeling effect. The activity was measured at 465°C after steady-state conditions were reached. Conversion was less than 10%. The products were analyzed by gas chromatography.

RESULTS

Acidity

Table 1 reports the results of the tests with colored indicators. They indicate an increase in acid strength as potassium ions are exchanged when the ion content is less than 1.7 K^+ per unit cell. The good correlation of this result with the following on ammonia and pyridine desorption confirms that surface acidity reflects bulk acidity.

Typical ir spectra obtained with pyridine in the 1650–1400 cm^{-1} region are reported in Fig. 1. Pyridinium ions absorb at 1540 cm^{-1}. The band at 1485 cm^{-1} is related to the pyridine coordinated to Brønsted and Lewis sites. The 1440-cm^{-1} band may be related to pyridine interacting with the cations (*8*). Lewis-coordinated pyridine gives a band at 1450 cm^{-1}. As the pyridine desorption temperature is increased beyond 150°C a splitting of the

1450-cm^{-1} band occurs for the more exchanged samples and a new band appears at 1458 cm^{-1}. As the desorption temperature is raised, the intensity of the 1450-cm^{-1} band decreases while that of the 1458-cm^{-1} band increases up to 350°C. Both bands disappear at 500°C. Changes in the 1440-cm^{-1} band are reported in Fig. 2 as a function of cation content for two desorption temperatures. The pyridine-cation interactions would cancel near 0.5 K^+ per unit cell. The Brønsted and Lewis acidities are given in Figs. 3 and 4. Both acidities increase as the ion content is decreased. Disturbances are detected near the abscissa 1 K^+/u.c. In order to compare the respective changes in the three acidic bands an evaluation of the amount of pyridine desorbed (1540- and 1450-cm^{-1} bands) or adsorbed (1458-cm^{-1} band) between 250 and 350°C is reported in Table 2 for the range of low cation contents. Even if one takes into account the influence of the extinction coefficients of the bands, the values indicate a larger change in Brønsted acidity than in Lewis acidity.

The amount of NH_3 desorbed in mole per degree and per unit cell calculated from desorption results is given as a function of desorption temperature in Fig. 5

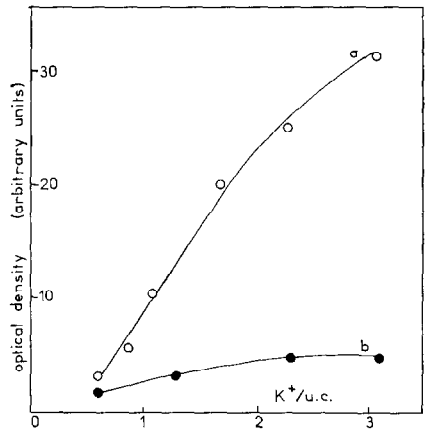

FIG. 2. Cation-bonded pyridine. Optical density of the 1440-cm^{-1} band as a function of potassium content. Pyridine evacuation at (a) 150; (b) 250°C.

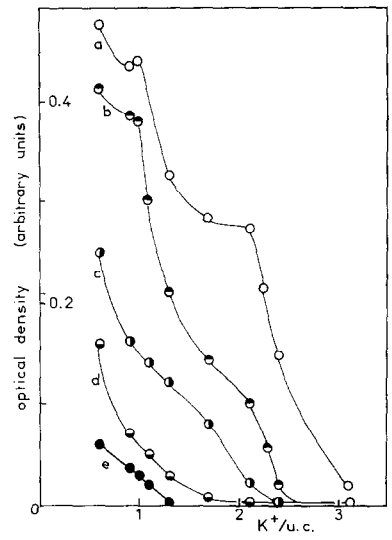

FIG. 3. Brønsted-bonded pyridine. Optical density of the 1540-cm^{-1} band as a function of cation content. Pyridine evacuation at (a) 150; (b) 250; (c) 300; (d) 350; (e) 380°C.

for NH_3 and Fig. 6 for pyridine. The shapes of the curves are similar for the two bases but the pyridine results are shifted to higher temperatures by 50 to 100°C. This might arise from the larger size of the pyridine molecule which diffuses more slowly and/or from different base–zeolite interactions. Since the process of desorption up to 400°C is more complete in the case of ammonia, only the ammonia results will be considered in detail. Figure 5 is completed by the results of Fig. 7 which reports the flow of ammonia molecules evolved evaluated in arbitrary units from the Pirani gauge

TABLE 2

Frequency (cm^{-1})	Nature of the site	Pyridine amount[a] (a.u.)	Reference curves
1540	Brønsted	−30	3b–3d
1450	Lewis	−2	4b–4c
1458	Lewis	+8	4c′–4b′

[a] Average difference in optical density of curves (column 4) of pyridine adsorbed (arbitrary units).

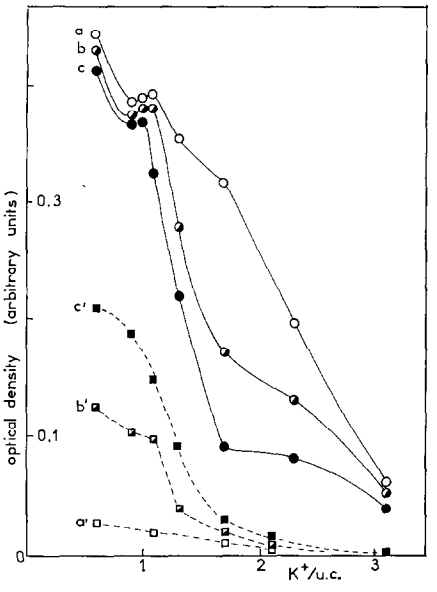

FIG. 4. Lewis-bonded pyridine. (a, b, c) Optical density of the 1450-cm^{-1} band and (a', b', c') the 1458-cm^{-1} band as a function of cation content. Pyridine evacuation at (a, a') 150; (b, b') 250; (c, c') 350°C.

pressure results. Due to the system geometry, the pressure measurements are less sensitive than weight losses for the separation of close desorption phenomena and only the envelope curve is obtained. This may be useful when secondary effects alter very much the desorption curves. Both types of curves in Figs. 5 and 7 detect two desorption ranges, the first one at temperatures below 110°C, the other one beyond 150°C. From Fig. 7 it appears in the second range that besides a continuous background due to ammonia desorption which increases in amount from the Of-3.1 to the Of-0.6 zeolite, specific desorption peaks start for all the zeolites near 160°C. A peak might be detected with a maximum near 200 to 230°C for the more cationated samples and a second peak whose maximum is near 260 to 310°C is present in the exchanged zeolites. The intensity and the shift of the peaks to high temperatures increase as ion content is decreased. Table 1 reports the peak maxima temperatures and the area of the peaks (amounts evolved) in arbitrary units evaluated from Fig. 7. Figure 8 reports in curve *a* the amount of ammonia evolved between room temperature and 110°C. Curves *b* and *c* give, respectively, the total amount of ammonia and pyridine desorbed in the chemisorption range (~110–400°C). For pyridine the desorption is carried out at 400°C for 24 hr up to a constant weight.

Both curves *b* and *c* lie slightly below the theoretical line which may be expected (curve *d*).

Catalytic Activity

The catalytic activity for isooctane cracking is reported in Fig. 9 as a function of ion content. It has been checked that the deactivation is small compared with what is usually observed with other zeolites (less than 8% of deactivation for the more active offretite after 5 hr compared to 50% for a similarly active zeolite Y). This is in agreement with the observed white color of offretite after 5 hr. The shape of the curve in Fig. 9 is similar to

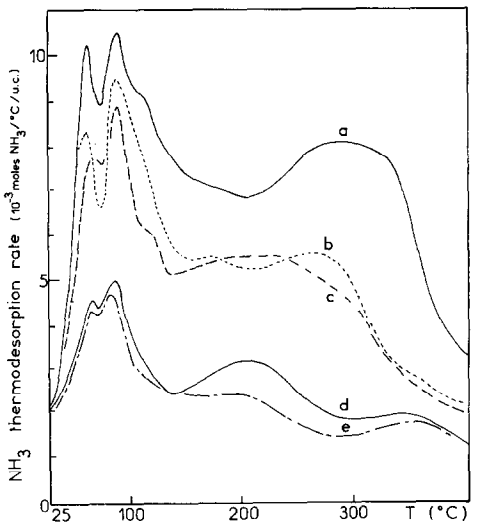

FIG. 5. Thermodesorption of ammonia from weight loss curves. (a) Of-0.6; (b) Of-1.1; (c) Of-1.3; (d) Of-2.1; (e) Of-3.1.

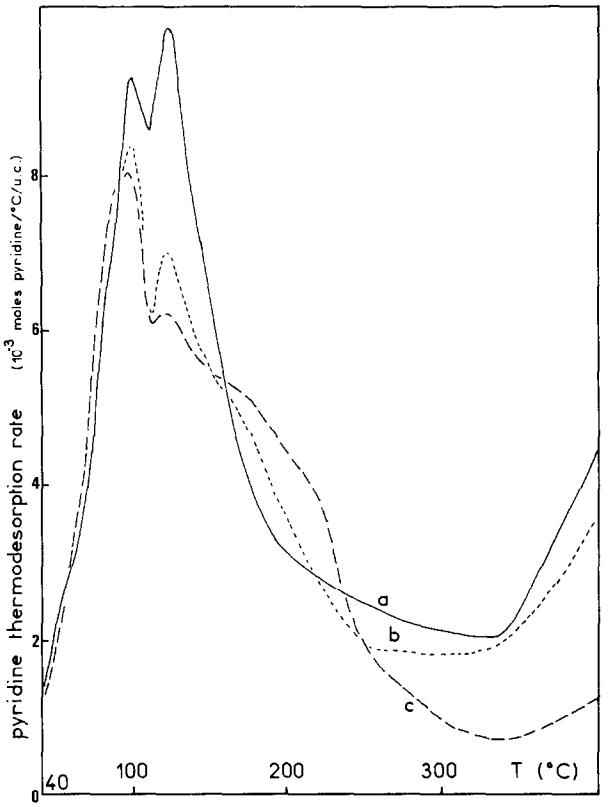

FIG 6. Thermodesorption of pyridine from weight loss curves. (a) Of-0.6; (b) Of-1.3; (c) Of-2.3.

that generally obtained with zeolites. The nearly amorphous sample Of-0.4 has a small activity. The other activity values give three steps in the curve. From 3.1 to 2.5 K^+/u.c. the activity is low and nearly constant. From 2.5 to 1 K^+/u.c. there is a linear increase of activity and finally a sharp rise occurs for the Of-0.6 sample. The main changes in product selectivity are given in Fig. 10. Three steps are also noted for 3.1 to 2.1; 2.1 to 1.3; 1.3 to 0.4 K^+/u.c. They differ from the previous ones detected on the activity curve. The selectivity given by the Of-0.4 sample is comparable to that of well-crystallized highly exchanged samples. From high to low cation content *trans*- and *cis*-butene-2 productions are not changed while the ratios of propene, isobutene, and isobutane are completely modified (Fig. 10). In order to try to relate the selectivity to a characteristic catalytic activity or a typical acidity, two offretite samples are compared in Table 3 with other zeolites giving similar isooctane conversion or having comparable acid strengths. No correlation is evident between selectivity and these two parameters.

DISCUSSION

Cation Location and Cage Accessibility

The TMA cations initially located in the gmelinite cages and the channels (*3*) are eliminated during the pretreatment at 550°C since no more νCH bands are observed in the 2800 to 3000-cm^{-1} ir region. As to the potassium ions it was postulated that each cancrinite cage contained one potassium ion (*1–3*, *5*) which could not be

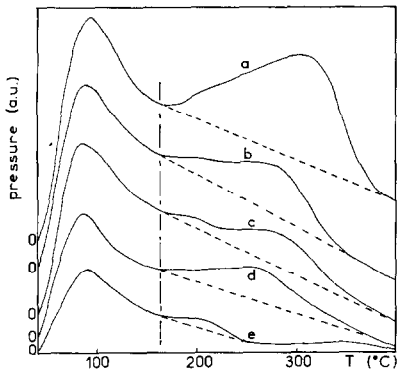

FIG. 7. Thermodesorption of ammonia from pressure measurements. (a) Of-0.6; (b) Of-1.3; (c) Of-1.7; (d) Of-2.1; (e) Of-3.1.

removed or exchanged without destroying the structure (*3*, *5*). This last point was not confirmed by the existence of well-crystallized offretite containing 0.9 and 0.6 K^+/u.c. (*6*). Since these remaining cations would be inaccessibly located in the cancrinite it is further surprising to obtain cation–pyridine interactions (Fig. 2). Due to the cancrinite cage aperture (maximum 1.8 Å) pyridine cannot enter the cavity. Since in the range 0.6 to 1 K^+/u.c. the cations are not easily exchangeable and hence seem to be strongly bonded to the framework it is very likely that pyridine attraction alone is not able to induce a cation migration. It is then inferred

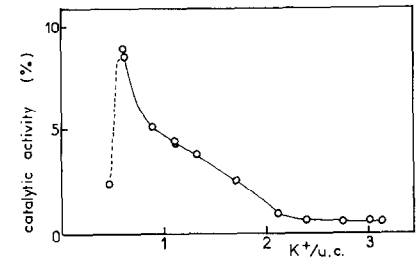

FIG. 9. Isooctane cracking at 465° as a function of cation content.

that the cations corresponding to 0.6 to 1 K^+/u.c. contents are not in the cancrinite cage. Either they were not in that cavity in the starting zeolite or more probably they have migrated upon chemical or thermal treatments without destroying the structure. Such a removal of cations from the cancrinite cage would induce some local disturbances in the properties, which are in fact observed in the Lewis and Brønsted acidity results (Figs. 3 and 4) near 1 K^+/u.c. The cation–pyridine interactions curve indicates a limit content of 0.5 K^+/u.c. in the cancrinite cage, cations which are inaccessible to pyridine. The other cations have been shown to be located in the gmelinite cage close to the cavity aperture (*3*). There are three such potential sites per unit cell (Fig. 11). It is then suggested that for

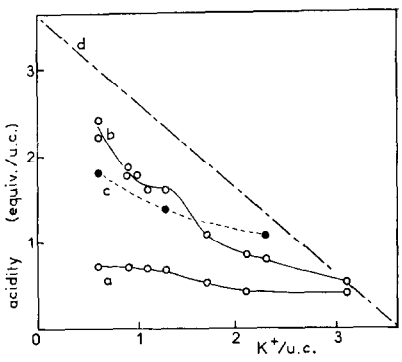

FIG. 8. (a, b) Thermodesorption of ammonia and (c) pyridine. Amount evolved in the temperature range (a) RT–110°; (b, c) 110–400°; (d) theoretical acid site number.

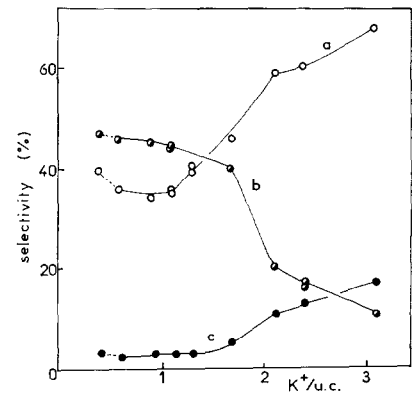

FIG. 10. Selectivity changes in isooctane cracking at 465°C as a function of cation content. (a) isobutene; (b) propene; (c) isobutane.

offretite samples with 0.5 K^+/u.c. all the gmelinite apertures are free of cations and one cancrinite cage in every two contains a cation. From ca. 0.5 to ca. 1.5 K^+/u.c. one gmelinite window per unit cell is progressively occupied. Between ca. 1.5 and 2.5 K^+/u.c. a second gmelinite aperture is occupied, and beyond 2.5 K^+/u.c. the third and last window of the gmelinite cavity is blocked. The values must be taken as an approximate estimate since there might be a statistical distribution of the cations. The cation location may change greatly the site accessibility. When only one window is cation free in some gmelinite cages (ion content higher than 2.5 K^+/u.c.) the adsorbed molecules may move only in the channel. If at least two gmelinite windows per cage have no cations the molecules may cross the gmelinite cage and move three-dimensionally in the framework (ion content lower than 2.5 K^+/u.c.). The range content 1.5 to 2.5 K^+/u.c. would be the more important for the changes from a one-dimensional to a three-dimensional circulation flow. The difference is not only a modification in the rate of diffusion but also the possibility for the diffusing molecules to reach sites in the gmelinite cage. Below 1.5 K^+/u.c. no new cavity becomes accessible. Such remarks may explain changes in various properties at these cation contents.

Looking first at Lewis acidity, previous results (*6*) have shown that the OH groups of exchanged offretite are stable at the pretreatment temperature (450°C). A dehydroxylation phenomenon cannot explain the large rise in Lewis acidity (1450- and 1458-cm^{-1} bands) observed near 1.5 K^+/u.c. in Fig. 4. The pyridine size (~6 Å) seems to be too large for the gmelinite window. However, it is known that aperture distortion may occur during the adsorption process of polar molecules (*2*). For instance, water molecules (kinetic diameter ~2.65 Å) may enter the cancrinite cages (*10*) whose openings are theoretically 1.8 Å (*1*). Therefore it is conceivable that pyridine might enter the gmelinite cage after cation exchange, hence increasing the number of measured Lewis sites.

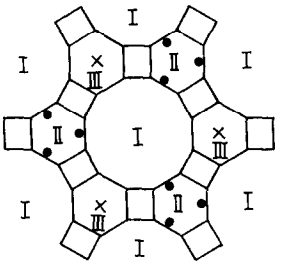

FIG. 11. Projection of offretite structure along *c* axis. Si or Al atoms are centered at each apex. Oxygen atoms lie about halfway between the apices. (I) channel; (II) gmelinite cage; (III) cancrinite or hexagonal prism. Cation sites: (●) gmelinite windows; (×) center of cancrinite cage.

The NH_3 thermodesorption shows two peaks in the range of physisorption at 65 and 90°C. They are proposed to be related to the desorption of ammonia from the channel and from the gmelinite cavity, re-

TABLE 3

Catalysts	Maximum pyridine desorption temperature (Brønsted acidity)	Isooctane cracking (% at 465°C)	Propene (%)	Isobutane (%)	Isobutene (%)	*cis* + *trans* butene (%)
NaHY 7.5	<350	4.0	19	17	51	13
Of-1.1	>380	4.2	44	4	35	17
NaMgHY 46.1	>350	8.0	2	49	32	17
Of-0.6	>380	9.0	45	2	35	18

spectively. In the range 2.1 to 1.3 K^+/u.c. the amounts desorbed are significantly increased for both physically (curve 8a) and chemically (curve 8b) bonded ammonia. This probably arises from a better accessibility of the gmelinite cages to ammonia. The very large amount of ammonia desorbed from the Of-0.6 sample at high temperature (Figs. 7a and 8b) may be explained by ammonia molecules entering the cation-free cancrinite cages.

The changes in selectivity shown in Fig. 10, which due to the small extent of deactivation cannot be related to coking, occur in the same intermediate potassium content range. There would be a selectivity characteristic of isooctane cracking in the channel (K^+ content > 2.5/u.c.) with a high C_4/C_3 ratio and a selectivity characteristic of catalysis in the channel and the gmelinite cavity with a high C_3/C_4 ratio (K^+ content < 1.5/u.c.). The intermediate selectivity values are explained by the increasing number of gmelinite cages becoming accessible for catalysis. It was shown that propene and isobutane arise from isobutene which is the primary cracking product (*11*). Table 3 indicates that the propene and isobutane production cannot be related to the extent of cracking or to the acid strength of the catalyst but rather to the zeolite type. It is then proposed that in highly exchanged offretites, propene and methane are formed at the expense of isobutane in gmelinite cavity where the steric hindrance and probably the expected high cavity field would promote a deeper cracking of C_4 molecules into C_1 and C_3 lighter hydrocarbons.

Acidity

Since Lewis acid sites retain pyridine at temperatures higher than the limit heating temperature of thermodesorption, it is very likely that thermodesorption reveals for a large part mainly Brønsted acidity. The pyridine values in Fig. 8 are lowest at low cation content. This could arise from the more difficult diffusion of pyridine. A long time is necessary to reach the weight equilibrium.

The number of both protonic and Lewis sites is raised upon cation exchange (Figs. 3 and 4). This probably results from the generation of sites and from the increasing accessibility of gmelinite cavities. As to the pyridine-Lewis 1458-cm^{-1} band formed upon heating with the more exchanged materials, such "high frequency" Lewis bands have been observed in Y zeolites (*7*, *12*), Na mordenite (*13*), and silica–alumina (*14*). It was suggested that the band arises from a species formed at high temperature from the pyridine already bonded to the solid (*14*). In offretites, the results of Table 2 allow some specific conclusions to be drawn: (i) the increase in the 1458-cm^{-1} band is not counterbalanced by a decrease of the 1450-cm^{-1} band. Thus the two Lewis acidities do not seem to be connected; (ii) there is no (or little) transformation of Brønsted acidity into the 1450-cm^{-1} Lewis acidity by dehydroxylation during pyridine desorption; (iii) the decrease in the 1540-cm^{-1} band is appreciably higher than the increase in the 1458-cm^{-1} band. Then assuming that the 1458-cm^{-1} Lewis sites arise from dehydroxylated Brønsted sites, only a part of the Brønsted sites should be dehydroxylated during pyridine desorption. The corresponding hydroxyl groups would be the less stable and would be generated at low cation contents. Such properties and previous results (*6*) suggest that the 1458-cm^{-1} Lewis sites would come from the dehydroxylation of the 3550-cm^{-1} hydroxyls by pyridine.

The acid strength changes with ion content are shown in colored indicators, thermodesorption, and ir studies. They all indicate a strength increase at low cation level. The weak acid sites formed during the exchange of the potassium cations of the first gmelinite window would give the

peak near 200 to 230°C observed in thermodesorption curves (Fig. 7, Table 1). The amount of base desorbed from weak Brønsted sites between 150 and 250°C evaluated from ir curves 3a and 3b being nearly constant as a function of potassium content, no more weak acid sites are formed upon further cation removal. The second thermodesorption peak (260–310°C) characterizes stronger sites whose strength increases as potassium cations are replaced by protons. These sites are stronger than in faujasites. They still adsorb pyridine at 380°C. The weak 1450-cm^{-1} Lewis sites are formed simultaneously with strong sites at the beginning of the cation exchange. For both Lewis site types ir studies indicate that the exchange of the two last cations of gmelinite windows and further the cation in the cancrinite cage give rise only to strong acidity. The sites retain pyridine up to 500°C.

Catalysis

Selectivity and catalytic activity do not depend on the same parameters. It has already been shown that the selectivity in offretite depends on whether the catalytic reaction proceeds only in the channel or also in the gmelinite cavity. On the contrary, the extent of isooctane conversion does not seem to be related to this cage accessibility. It rather parallels, as generally observed in zeolites, the number of strong protonic acid sites as evaluated from ir experiments while the correlation with strong Lewis acidity is less good. It was previously shown that a large part of the Brønsted acidity of offretite arises from hydroxyl groups absorbing at 3610 cm^{-1} and located in the channel and the gmelinite cavity (*6*). Therefore it is inferred that the strongest of these protons are the catalytic active centers.

CONCLUSION

Compared to other zeolites, offretite is characterized by some special properties. The cations located in the gmelinite cage windows block the cage entrance. The progressive exchange of these cations allows the adsorbed molecules to only enter the gmelinite cavity where they are trapped or to diffuse through it. This changes the molecule flow from diffusing only along the channel or in a three-dimensional way. These modifications in cage accessibility are responsible for a typical selectivity giving a high C_3/C_4 ratio and little isobutane. Cracking of *n*-hexane in the inner cavities of erionite was also reported to favour C_3 products at the expense of isobutane (*4*). The activity of offretite is high compared to that of various faujasites. It may arise from its stronger acidity, from the high field in the small voids of offretite or from the influence of activity coefficients on the reaction rate (*15*). Due to the rather low Al content in offretite this coefficient would be higher than in Y zeolite.

ACKNOWLEDGMENT

We thank Professor R. M. Barrer for the gift of offretite samples.

REFERENCES

1. Whyte, T. E., Jr., Wu, E. L., Kerr, G. T., and Venuto, P. B., *J. Catal.* **20**, 88 (1971).
2. Gard, J. A., and Tait, J. M., *Advan. Chem. Ser.* **101**, 230 (1971).
3. Barrer, R. M., and Harding, D. A., *Separ. Sci.* **9**, 195 (1974).
4. Chen, N. Y., *in* "Proceedings 5th Int. Congr. Catalysis" (J. W. Hightower, Ed.), p. 1343. North–Holland, Amsterdam, 1973.
5. Gard, J. A., and Tait, J. M., *Acta Crystallogr. B* **28**, 825 (1972).
6. Mirodatos, C., Abou Kais, A., Vedrine, J. C., and Barthomeuf, D., *J. Chem. Soc. Faraday Trans. I* **74**, 1786 (1978).
7. Beaumont, R., Pichat, P., Barthomeuf, D., and Trambouze, Y., *in* "Proceedings 5th Int. Congr. Catalysis" (J. W. Hightower, Ed.), p. 343. North–Holland, Amsterdam, 1973.
8. Liengme, S. V., and Hall, W. K., *Trans. Faraday Soc.* **62**, 3229 (1966).

9. Breck, D. W., "Zeolite Molecular Sieves," p. 638. Wiley, New York, 1974.
10. Breck, D. W., and Grose, R. W., *Advan. Chem. Ser.* **121**, 319 (1973).
11. Barthomeuf, D., and Beaumont, R., *J. Catal.* **30**, 288 (1973).
12. Jacobs, P. A., and Uytterhoeven, J. B., *J. Catal.* **26**, 175 (1972).
13. Cannings, F. R., *J. Phys. Chem.* **72**, 4691 (1968).
14. Ballivet, D., Barthomeuf, D., and Pichat, P., *J. Chem. Soc. Faraday Trans. I* **68**, 1712 (1972).
15. Barthomeuf, D., *C.R. Acad. Sci.* **286C**, 181 (1978); *Acta Phys. Chem. nova ser. Szeged* **24**, 71 (1978).